

Masked and Permuted Implicit Context Learning for Scene Text Recognition

Xiaomeng Yang^{1,2}, Zhi Qiao³, Jin Wei⁴, Yu Zhou^{1,2*}, Ye Yuan³, Zhilong Ji³, Dongbao Yang^{1,2}, Weiping Wang¹

¹Institute of Information Engineering, Chinese Academy of Sciences, Beijing, China

²School of Cyber Security, University of Chinese Academy of Sciences, Beijing, China

³Tomorrow Advancing Life, Beijing, China

⁴Communication University of China, Beijing, China

{yangxiaomeng,zhouyu,yangdongbao,wangweiping}@iie.ac.cn

{qiaozhi1,yuanye8,jizhilong}@tal.com, weijin@cuc.edu.cn

ABSTRACT

Scene Text Recognition (STR) is a challenging task due to variations in text style, shape, and background. Incorporating linguistic information is an effective way to enhance the robustness of STR models. Existing methods rely on permuted language modeling (PLM) or masked language modeling (MLM) to learn contextual information implicitly, either through an ensemble of permuted autoregressive (AR) LMs training or iterative non-autoregressive (NAR) decoding procedure. However, these methods exhibit limitations: PLM’s AR decoding results in the lack of information about future characters, while MLM provides global information of the entire text but neglects dependencies among each predicted character. In this paper, we propose a Masked and Permuted Implicit Context Learning Network for STR, which unifies PLM and MLM within a single decoding architecture, inheriting the advantages of both approaches. We utilize the training procedure of PLM, and to integrate MLM, we incorporate word length information into the decoding process by introducing specific numbers of mask tokens. Experimental results demonstrate that our proposed model achieves state-of-the-art performance on standard benchmarks using both AR and NAR decoding procedures.

CCS CONCEPTS

• Applied computing → Optical character recognition.

KEYWORDS

Scene Text Recognition, OCR, Masked and Permuted Context Learning, Autoregressive, Non-autoregressive

1 INTRODUCTION

Scene text recognition (STR) [23, 52], aiming at recognizing sequential characters in natural scene images, has attracted more and more research interests because of its wide range of practical application values, such as robot navigation and street image understanding. Because of the variations of scene text in style, shape, and background, only using visual features limits the performance of STR. Since texts contain rich linguistic information, numerous methods have been exploring how to incorporate linguistic knowledge into STR models.

Traditionally, STR methods utilize the recurrent attention mechanism to capture linguistic information of the text during the decoding process [2, 34]. However, the left-to-right autoregressive (AR)

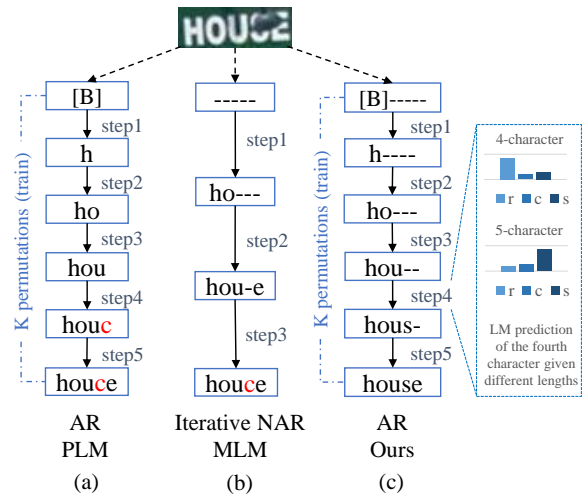


Figure 1: Decoding procedures of PLM, MLM, and our unified language modeling. Our unified language modeling is trained with permuted AR decoding but could obtain general linguistic information as well. “-” in the figure represents the mask token used in decoding. The lack of global information and inadequate linguistic learning leads to misrecognition of PLM and MLM based methods.

decoder can only get limited one-way serial linguistic context. To address these limitations, prior works take advantage of the external transformer-based language model (LM) [26, 50]. They decouple the vision model (VM) and LM, which take the prediction of the VM as input and rectify the visual prediction based on the learned linguistic knowledge. The external LM of ABINet [10] obtains the global information from VM’s initial prediction and learns context between each characters. Although STR models with external LM achieve promising performance, the independence between VM and LM causes problems. [3] proves that the conditional independence between VM and LM may cause erroneous rectification for the correct predictions from VM. Furthermore, PETR [45] shows that the low character-wise accuracy of VM and inaccurate word length of visual prediction limit the LM’s performance. Thus, an internal LM able to influence the visual space may be a better choice.

Inspired by the permuted language modeling (PLM) [47] or masked language modeling (MLM) [7] techniques in natural language processing, previous methods have designed creative decoder modules to extract linguistic information. PARSeq [3] employs an ensemble of permuted autoregressive LMs to learn an internal LM. However, the AR decoder’s character-by-character decoding limits the learned LM’s ability to anticipate future characters or grasp global information. As illustrated in Figure 1(a), when recognizing the fourth character in the word “house”, the model lacks knowledge of the remaining characters. Consequently, it can only determine the character based on the preceding three characters “hou” and the ambiguous visual features present in the image, which leads to the misrecognition of the character “c” instead of the correct “s”. Besides, although the PLM training strategy permits non-autoregressive inference, its performance falls short compared to AR inference due to the absence of explicit contextual information. On the contrary, the MLM-based methods could provide general positional information about the entire text for linguistic learning but may neglect dependency among each predicted character. PIMNet [30] iteratively determines the length of the word to provide global positional information for subsequent iterations, but it could only learn the context between characters predicted in different iterations. This approach lacks contextual knowledge among characters predicted within the same iteration, such as “h” and “o” both determined in Figure 1(b), which are predicted simultaneously in the first iteration. Consequently, the internal LM learned by PIMNet is insufficient and constrained by the images present in the training dataset. In summary, both language modeling approaches have inherent limitations that affect the performance and capability of the learned decoder with internal LMs. To improve STR performance, a more comprehensive linguistic information acquisition method is needed. Our goal is to enable the model to learn richer linguistic information implicitly during training, which would facilitate both AR and NAR inference while reducing the performance gap between them.

Based on the above analysis, we propose a Masked and Permuted Implicit Context Learning STR (MPSTR for short) method to learn an internal LM with superior linguistic information. Inspired by [36], we adapt the unified language modeling approach for STR, combining PLM and MLM into a single framework by rearranging tokens. The training procedure follows PLM, with several mask tokens appended after the predicted characters, before each AR decoding of all permutations. These tokens provide global context information for linguistic learning, as depicted in Figure 1(c). During training, MPSTR predicts each character in an AR fashion to model character dependencies while incorporating mask tokens in each iteration to represent remaining characters, offering a global context. For instance, by utilizing the information that we are predicting the fourth character in a five-character word, combined with the preceding “hou” and visual features, our MPSTR is capable of predicting the correct “s” during the fourth iteration. Additionally, the single PLM decoder attends solely to previous tokens during inference, ensuring that randomly predicted characters following the ending symbol do not impact its prediction. However, when incorporating MLM with redundant mask tokens, determining the valid length of the target text becomes crucial. We introduce an explicit length prediction procedure to our model using a simple learnable length token that minimally impacts memory burden.

Specifically, the number of appended mask tokens corresponds to the number of un-transcribed characters in the current iteration. This approach enables the decoder to attain more precise global linguistic information. To address potential inaccuracies in length prediction, we incorporate a length perturbation during training, enhancing our model’s robustness.

Furthermore, our approach intends to learn an advanced internal LM through uniquely incorporates mask tokens and length information to provide global linguistic knowledge at each decoding step, unifying PLM and MLM into a single framework for STR. This differs from previous methods [16, 19, 46] which directly using the length as an additional supervision.

We conduct extensive experiments to evaluate our proposed method. Compared to the PLM-based ParSeq and MLM-based PIMNet, our MPSTR demonstrates superior performance on public benchmarks. In AR decoding, MPSTR outperforms ParSeq by 0.6% and 0.3% when trained on synthetic and real datasets, respectively. When employing NAR decoding for inference, MPSTR surpasses PARSeq and PIMNet with improvements of approximately 0.7% and 1.2% when trained on synthetic datasets, and 0.9% and 1.9% when trained on real datasets.

The contributions of this work are summarized as follows:

- We propose a model that leverages the unification of PLM and MLM in a single decoding architecture, inheriting their advantages and providing superior linguistic information during the recognition process.
- To integrate MLM, we employ a simple yet effective length-prediction method using a learnable token in the ViT encoder, along with perturbed training, which enhances the quality of global context information.
- Noticing that there are mislabeled images in benchmark datasets, we conduct verification of the labels to ensure a more accurate evaluation of scene text recognition models: github.com/Xiaomeng-Yang/STR-benchmark-cleansed.
- Our proposed model achieves state-of-the-art (SOTA) performance on standard benchmarks using both AR and NAR decoding procedures. Notably, with NAR inference, it outperforms both PLM-based and MLM-based text recognizer by a significant margin.

2 RELATED WORK

As a long-term research topic, scene text recognition (STR) has made great progress over the years [4, 27, 28, 42, 48, 49]. Our paper primarily focuses on the linguistic knowledge learning for STR, so we divide STR methods into two categories, language-free and language-aware methods, depending on whether linguistic information is applied.

2.1 Language-Free STR

Language-free methods focus on the visual information of scene text images and do not consider the contextual relationship between characters. Connectionist Temporal Classification (CTC) [11] based methods [14, 22, 33] primarily extract visual features using a convolutional neural network (CNN) and then build sequence modeling through a recurrent neural network (RNN). These methods generate predictions for each frame of the feature sequence without

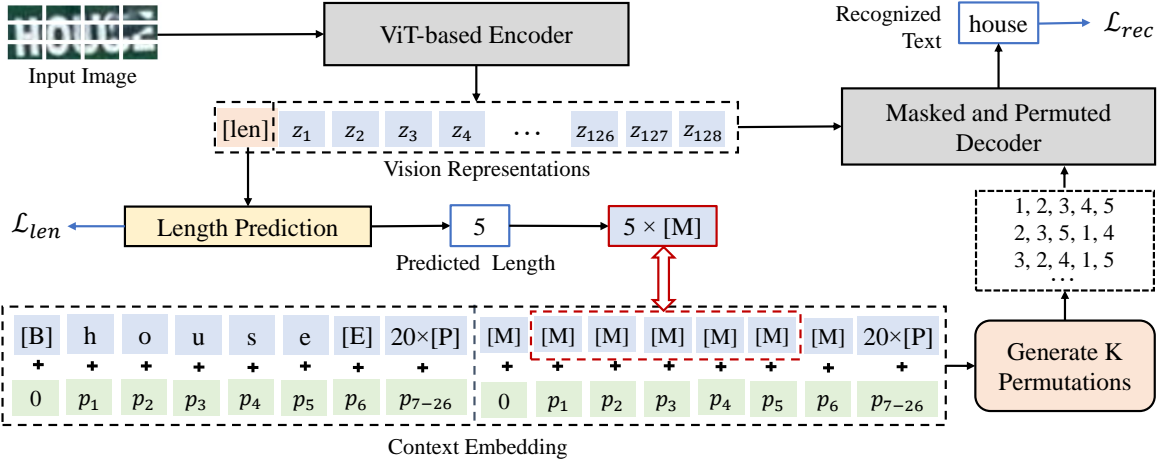


Figure 2: Architecture of the proposed method. $[B]$, $[E]$, $[P]$ and $[M]$ stands for the beginning-of-sequence, end-of-sequence, padding and mask tokens, respectively. The ViT-based encoder provides the text length using the $[len]$ token. Then, the predicted length number of mask tokens are appended. After K permutation operations, the masked and permuted text is input to the decoder for the corresponding prediction.

taking the conditional dependencies between characters into account. Segmentation-based models [12, 21, 41] employ semantic segmentation at the character level and subsequently group the segmented characters into words. Drawing inspiration from the success of the Vision Transformer (ViT) [8], which uses the Transformer [39] architecture for image feature extraction, ViTSTR [1] adapts the ViT for STR. This approach directly decodes the visual representations learned by the ViT encoder in a non-autoregressive manner. However, language-free STR methods tend to perform poorly when recognizing low-quality images due to the absence of linguistic information.

2.2 Language-Aware STR

Initially, attention-based methods [2, 20, 34] were employed to obtain linguistic information in text by learning internal LMs with an AR decoder. However, these methods could only capture serial context. SEED [31] addressed this limitation by utilizing a pre-trained language model to guide the AR decoder. Recently, more-advanced methods have been developed to learn external or internal LMs based on the Transformer architecture. Models with external LMs [10, 50] propose semantic modules to learn semantic knowledge and refine initial predictions from the vision backbone. LevOCR [6] further investigates how to fuse visual and linguistic features effectively. To learn an internal LM at the vision level, VisionLAN [44] introduces a visual reasoning module that randomly masks corresponding visual features of characters during training. SVTR [9] designs local and global mixing blocks for a ViT-based encoder to capture both intra-character and inter-character dependencies. MGP-STR [43] incorporates subword representations to enable multi-granularity prediction. PTIE [37] trains an ensemble of the same architecture, consisting of a ViT encoder and a transformer decoder, with different patch resolutions and AR decoding

directions. Inspired by MLM, PIMNet [30] employs an easy-first decoding strategy, which iteratively performs NAR decoding and obtains contextual information between characters predicted in different iterations. PARSeq [3] learns an internal LM using PLM instead of the standard AR modeling, but its linguistic knowledge learning process disregards global positional information. In this paper, we aim to achieve better implicit context learning by inheriting the advantages of both PLM and MLM in a single decoder.

3 METHOD

The proposed method, as illustrated in Figure 2, comprises a ViT-based encoder and a Masked and Permuted Decoder (MP-decoder). The encoder is responsible for extracting visual features from the input image and predicting the length of the word. Subsequently, the MP-decoder employs the unification of MLM and PLM to decode the visual representations into the final predicted text with context embedding. This unified approach takes advantage of both MLM and PLM, allowing the model to effectively learn and leverage contextual information during the decoding process.

3.1 ViT-based Encoder and Length Prediction

The encoder is based on ViT, which takes image patches as input and extracts visual features using Multi-head Self-Attention, Layer Normalization (LN), Multi-layer Perceptron (MLP) and residual connections. As depicted in Figure 2, the input image $\mathbf{x} \in \mathbb{R}^{H \times W \times C}$ is divided into $P_w \times P_h$ patches. Then, $N = HW / (P_w P_h)$ patches are flattened into vectors and linearly projected into D -dimensional tokens. Instead of the original $[class]$ token in ViT backbone, we introduce a learnable $[len]$ token for length prediction. Additionally, position embeddings of equal dimension are added to each token to retain the positional information of the image patches. The final

generated patch embedding vector is:

$$\mathbf{z}_{input} = \left[\mathbf{x}_{length}; \mathbf{x}_p^1 \mathbf{E}; \mathbf{x}_p^2 \mathbf{E}; \dots; \mathbf{x}_p^N \mathbf{E} \right] + \mathbf{E}_{pos} \quad (1)$$

where $\mathbf{x}_{length} \in \mathbb{R}^{1 \times D}$ is the embedding of $[len]$, $\mathbf{E} \in \mathbb{R}^{(P_h P_w) \times D}$ is the patch embedding matrix and $\mathbf{E}_{pos} \in \mathbb{R}^{(N+1) \times D}$ is the position embedding.

Given $\mathbf{z}_{input} \in \mathbb{R}^{(N+1) \times D}$, the 12-layer ViT encoder outputs the final embedding $\mathbf{z} = [z_0, z_1, z_2, \dots, z_{N-1}, z_N]$. We use z_0 to predict the length of the word L with LN, two fully connected layers (FC) and an argmax layer. The word length prediction is treated as a T -class classification task, where T represents the maximum possible length.

$$L = \text{argmax}(\text{FC}(\text{LN}(z_0))) \quad (2)$$

The other learned tokens $\mathbf{z}_v = [z_1; z_2; \dots; z_N]$ are used as input vision representations for the MP-decoder.

3.2 Masked and Permuted Language Modeling

Masked and permuted language modeling aims to combine the advantages of PLM and MLM. Let \mathcal{Z}_T represent all possible permutations of the index $[1, 2, \dots, T]$. A PLM-based method trains the transformer decoder by maximizing the following likelihood:

$$\log p(\mathbf{y}|\mathbf{x}) = \mathbb{E}_{\mathbf{z} \sim \mathcal{Z}_T} \left[\sum_{t=1}^T \log p_{\theta}(y_{z_t} | y_{z_{<t}}, \mathbf{x}) \right] \quad (3)$$

where z_t and $z_{<t}$ denote the t -th character and the previous $t-1$ characters in the specific permutation \mathbf{z} . In other words, a PLM-based decoder predicts the characters one-by-one depending on the determined ones, in the order of each permutation.

MLM-based methods replace several tokens with mask tokens and generate the masked characters depending on context between the masked and unmasked characters in a NAR way. Let \mathcal{K}_i represent the set of masked positions in iteration i , $y_{\mathcal{K}_i}$ be the set of masked tokens, $y_{\setminus \mathcal{K}_i}$ be the tokens after masking, and I be the number of iterations. An iterative MLM-based NAR decoder maximizes the following objective:

$$\log p(\mathbf{y}|\mathbf{x}) \approx \sum_{i=1}^I \sum_{k \in \mathcal{K}_i} \log p_{\theta}(y_k | y_{\setminus \mathcal{K}_i}, \mathbf{x}) \quad (4)$$

To unify PLM and MLM, we consider the c -th step of AR decoding in PLM for a specific permutation, where characters $y_{z_{<c}}$ have been generated. Suppose that the MLM decoder masks characters $y_{z_{\geq c}}$ for an iteration, it could predict the masked tokens depending on the predicted $y_{z_{<c}}$ and mask tokens $\mathbf{M}_{z_{\geq c}}$ in parallel. Thus, we can unify them into one decoder such that when generated next character autoregressively in each permutation, the unified MP-decoder should depend on both the predicted part and several mask tokens whose number is equal to the number of remaining undetermined characters. The unified training objective of MP-decoder is formulated as :

$$\mathbb{E}_{\mathbf{z} \sim \mathcal{Z}_T} \left[\sum_{t=c}^T \log p_{\theta}(y_{z_t} | y_{z_{<t}}, \mathbf{M}_{z_{\geq c}}, \mathbf{x}) \right] \quad (5)$$

This inherits the ensemble of permuted AR decoding training process from PLM and mask tokens' information for unpredicted characters like MLM.

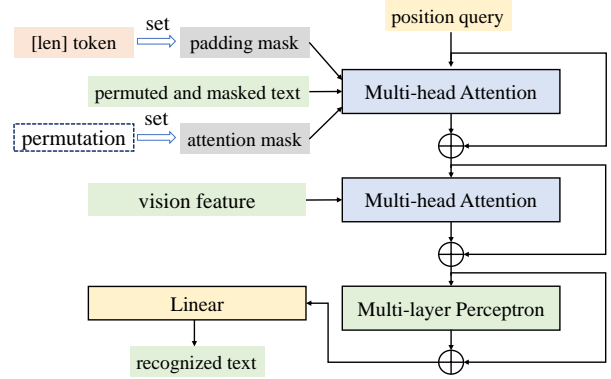


Figure 3: The architecture of Masked-Permuted Decoder (MP-decoder).

3.3 Masked and Permuted Decoder

The pipeline of MP-decoder is shown in Figure 3, which adopts two Multi-Head Cross-Attention (MHCA) modules.

The first MHCA receives position query $\mathbf{p} = [p_1; p_2; \dots; p_{T+1}]$ with length $T+1$ for an additional $[EOS]$ token and context embedding \mathbf{c} as key and value:

$$\mathbf{h}_c = \mathbf{p} + \text{MHCA}(\mathbf{p}, \mathbf{c}, \mathbf{c}, \mathbf{m}_{attn}, \mathbf{m}_{pad}) \quad (6)$$

where $\mathbf{c} = [\mathbf{c}_{word}; \mathbf{c}_{mask}] \in \mathbb{R}^{2(T+2) \times D}$ is the concatenation of word context embeddings $\mathbf{c}_{word} \in \mathbb{R}^{(T+2) \times D}$ and mask context embeddings $\mathbf{c}_{mask} \in \mathbb{R}^{(T+2) \times D}$, both of which are added with positional information as shown in Figure 2. $\mathbf{m}_{attn} \in \mathbb{R}^{(T+1) \times 2(T+2)}$ and $\mathbf{m}_{pad} \in \mathbb{R}^{2(T+2)}$ are the attention mask for permutation and padding mask, respectively.

Since we cannot train on all $L!$ permutations, we choose K permutations from \mathcal{Z}_L , and the chosen permutations are informed to the decoder through the attention mask. The attention mask $\mathbf{m}_{attn} = [\mathbf{m}_{wattn}; \mathbf{m}_{mattn}]$ is generated uniquely for each chosen permutation according to equation (5), where \mathbf{m}_{wattn} and \mathbf{m}_{mattn} are attention masks for \mathbf{c}_{word} and \mathbf{c}_{mask} , respectively. Specifically, at a certain step of AR decoding, the unpredicted part of the word context embeddings and the mask context embeddings corresponding to the predicted tokens are masked, e.g. the example in Table 1. When decoding the character y_3 , $[B]$ and y_1 in \mathbf{c}_{word} , and the last three $[M]$ in \mathbf{c}_{mask} could be attended. The padding mask is determined by the predicted word length L with first $L+2$ tokens unmasked for both \mathbf{c}_{word} and \mathbf{c}_{mask} . In other words, $\mathbf{m}_{pad} = [\mathbf{m}_{wpad}; \mathbf{m}_{mpad}]$, where $\mathbf{m}_{wpad} = \mathbf{m}_{mpad}$. For example, for the word "house" with length 5, $\mathbf{m}_{wpad} = \mathbf{m}_{mpad} = [1, 1, 1, 1, 1, 1, 0, \dots, 0] \in \mathbb{R}^{T+2}$.

The second MHCA computes the attention \mathbf{h}_i between \mathbf{h}_c and image visual features \mathbf{z}_v obtained from the ViT encoder. The prediction is ultimately achieved by processing the output logits through a MLP and a FC layer.

$$\mathbf{h}_i = \mathbf{h}_c + \text{MHCA}(\mathbf{h}_c, \mathbf{z}_v, \mathbf{z}_v) \quad (7)$$

$$\mathbf{y} = \text{FC}(\mathbf{h}_i + \text{MLP}(\mathbf{h}_i)) \quad (8)$$

Table 1: The attention mask m_{attn} for permutation[1, 3, 2]. The table header represents the tokens for context embeddings c , while the header column represents the tokens being decoded at each step. 1 means the token in the table header is masked when decoding the corresponding token in the header column.

	[B]	y_1	y_2	y_3	[E]	[M]	[M]	[M]	[M]	[M]
y_1	0	1	1	1	1	1	0	0	0	0
y_2	0	0	1	0	1	1	1	0	1	0
y_3	0	0	1	1	1	1	1	0	0	0
[E]	0	0	0	0	1	1	1	1	1	0

Table 2: The AR inference attention mask for left-to-right decoding. A value of 0 indicates that when decoding the token in the header column, the query can attend to the corresponding token in the table header.

	[B]	y_1	y_2	...	y_L	[E]	[M] ₀	[M] ₁	[M] ₂	...	[M] _L	[M] _{L+1}
y_1	0	1	1	1	1	1	1	0	0	0	0	0
y_2	0	0	1	1	1	1	1	1	0	0	0	0
...	0	0	0	1	1	1	1	1	1	0	0	0
y_L	0	0	0	0	1	1	1	1	1	1	0	0
[E]	0	0	0	0	0	1	1	1	1	1	1	0

3.4 Training Objective and Strategies

The objective function of our proposed method is formulated as follows:

$$\mathcal{L} = \lambda \mathcal{L}_{len} + (1 - \lambda) \mathcal{L}_{rec} \quad (9)$$

where \mathcal{L}_{len} represents the loss of length prediction, and \mathcal{L}_{rec} stands for the recognition loss. The parameter λ is employed to balance the two losses. We treat the length prediction as a T -class classification task (where T is the set maximum length) and use cross-entropy loss for \mathcal{L}_{len} . Let p_{len} and g_{len} denote the predicted word length and ground truth word length respectively, and L_{ce} represent the cross-entropy loss.

$$\mathcal{L}_{len} = L_{ce}(p_{len}, g_{len}) \quad (10)$$

For recognition loss, we compute the mean of the cross-entropy losses between predicted text y_k and ground truth label \hat{y} for K chosen permuted decoding orders.

$$\mathcal{L}_{rec} = \frac{1}{K} \sum_{k=1}^K L_{ce}(y_k, \hat{y}) \quad (11)$$

During training, we employ a teacher forcing strategy, using the ground truth length g_{len} to set the mask tokens, which aids in learning advanced contextual information among characters. For inference, the predicted length L is used. Additionally, to enhance the robustness of the decoder for predicted length, we introduce perturbation to g_{len} for a proportion of images in a batch, such as $g_{len} - 1$ or $g_{len} + 1$. The perturbed length is then randomly utilized to determine the number of mask tokens.

4 EXPERIMENTS

4.1 Datasets

For a fair comparison, we utilize MJSynth [15] and SynthText [13] as our synthetic (S) training data, and real text images collected by [3] as real (R) training data. We test the models on six widely-used public benchmarks: IIIT 5k-word (IIIT5k) [25], which comprises 3,000

high-quality website images; ICDAR 2013 (IC13) [18], containing either 1,015 or 857 images (the latter excludes images with words less than three characters); Street View Text (SVT) [42], consisting of 647 images from the Google Street View; ICDAR 2015 (IC15) [17] featuring 2,077 unfocused images captured by Google Glass (some researchers use a 1,811-image version that omits extremely distorted images); SVT-Perspective (SVTP) [29], with 645 test word images from the Google Street View; and CUTE80 (CUTE) [32], which includes 288 high-quality curved images.

However, there are mislabeled images in test benchmark [2]. Despite the widespread use of these datasets, label noise has received little attention. State-of-the-art models have achieved a remarkable 96% accuracy on the benchmark using real training data. Testing the models on a cleansed label set is crucial for obtaining their true performance and avoiding potential negative optimization. To address this issue, we utilize the cleansed labels from [2] and conduct further verification of these labels. Detailed information can be found in our supplementary file.

In addition to the six benchmark datasets, we also conduct experiments on three more challenging datates: COCO-Text [40], comprising 9.8k samples, most of which are occluded and distorted; ArT [5], containing 35.1k curved and rotated hard-case images; Uber-Text [51], which consists of 80.6k samples featuring vertical and rotated text.

4.2 Implementation Details

4.2.1 Model Configuration. Following recent STR methods [3, 43], our configuration for the ViT encoder is similar to DeiT [38], which consists of 12 transformer blocks. Our MPSTR employs the DeiT-small configuration, featuring 6-head attention and a 384-dimension embedding. The input image size is set to 128×32 , and the patch size is 8×4 . We set the maximum length T to 25. Our model predicts a 36-character charset, including 10 digits and 26 alphabets, as well as an ending symbol.

Table 3: Results on six benchmark datasets with cleansed label. For methods releasing pretrained weights, we directly evaluate them on the cleansed benchmark. * indicates that the models are reproduced by us. We follow the official configuration for PARSeq and change the backbone of PIMNet to DeiT-small for fair comparison. MGP-STR[†] represents the small model performance for fair comparison. S¹ LM pretrained on WikiText-103 [24]. “N” and “A” are NAR and AR decodings. The inference time is averaged over 7,672 images.

Method	Train Data	IIIT5K		IC13		SVT		IC15		SVTP		CUTE		Average		Params. (M)	Time (ms/image)
		3000	857	1015	647	1811	2077	645	288	7248	7672	7248	7672				
TRBA [2]	S	90.5	93.3	92.7	87.3	79.0	74.4	78.5	72.9	85.9	84.5	49.6	16.7				
ViTSTR [1]	S	88.9	92.6	91.8	87.2	80.5	74.7	82.3	80.9	86.2	84.5	85.5	7.92				
SRN [50]	S	92.2	95.2	93.7	89.6	81.7	77.2	85.1	88.5	88.9	87.4	54.7	12.1				
VisionLAN [44]	S	96.5	96.3	94.5	90.4	85.4	81.3	85.7	88.9	91.9	90.4	32.8	14.8				
PIMNet* [30]	S	95.5	95.9	95.0	92.0	86.5	82.2	87.9	90.6	92.1	90.7	30.1	15.6				
ABINet [10]	S ¹	97.0	97.0	95.2	93.4	87.3	83.4	89.6	89.2	93.3	91.9	36.7	23.4				
MGP-STR [†] [43]	S	95.6	96.6	95.7	93.0	87.8	83.6	89.0	88.5	92.7	91.3	52.6	9.37				
PARSeq _N * [3]	S	96.0	96.6	95.7	92.4	86.8	83.1	88.7	90.6	92.6	91.4	23.8	11.7				
PARSeq _A * [3]	S	96.6	97.0	96.1	92.7	87.8	84.2	<u>89.3</u>	91.7	93.3	92.0	23.8	17.5				
LevOCR [6]	S	<u>97.1</u>	96.7	95.5	94.4	<u>88.4</u>	<u>84.6</u>	89.6	<u>90.6</u>	<u>93.7</u>	<u>92.4</u>	92.6	60.5				
MPSTR _N (Ours)	S	96.8	96.4	95.4	92.6	88.2	84.3	88.5	91.7	93.3	92.0	23.8	12.6				
MPSTR _A (Ours)	S	97.2	<u>96.9</u>	<u>95.9</u>	<u>93.2</u>	89.0	85.3	89.6	91.7	93.9	92.6	23.8	19.1				
PIMNet* [30]	R	97.7	97.1	97.0	96.5	90.9	89.2	92.9	95.1	95.3	94.7	30.1	15.6				
PARSeq _N [3]	R	98.1	97.9	98.1	97.2	92.8	91.6	94.0	98.6	96.3	96.0	23.8	11.7				
PARSeq _A [3]	R	98.9	<u>98.3</u>	98.5	97.5	<u>93.7</u>	<u>92.6</u>	<u>95.7</u>	<u>98.6</u>	97.1	96.7	23.8	17.5				
MPSTR _N (Ours)	R	<u>99.0</u>	98.4	<u>98.4</u>	<u>98.3</u>	<u>93.7</u>	92.4	95.5	<u>98.6</u>	<u>97.2</u>	<u>96.8</u>	23.8	12.6				
MPSTR _A (Ours)	R	99.2	<u>98.3</u>	98.3	98.5	93.9	92.7	96.1	99.0	97.4	97.0	23.8	19.1				

4.2.2 Model Training. We use two GPUs to train our models. MPSTR is trained with 384 batch size. Data augmentations like Gaussian blur, Poisson noise and rotation are randomly performed the same with PARSeq [3]. The Adam optimizer is adopted with 1cycle [35] learning rate scheduler for the 85% of training iterations and Stochastic Weight Averaging scheduler for the remaining part. We set $K = 12$ permutations and $\lambda = 0.25$. All models are trained for 254,520 iterations.

4.2.3 Model Evaluation. For evaluation, we follows the set of [3] using AR decoding with one refinement iteration and NAR decoding with two refinement iterations. The refinement is performed using the cloze mask.

The NAR decoding generates all tokens simultaneously with all position queries $\mathbf{p} = [\mathbf{p}_1, \mathbf{p}_2, \dots, \mathbf{p}_{T+1}]$, where T is the maximum length, and \mathbf{p}_{T+1} is added for the end-of sequence (eos) token. For NAR inference, we provide the beginning token $[B]$ along with $L + 2$ mask tokens $[M]$, where $[M]_0$ and $[M]_{L+1}$ represents the corresponding mask tokens for beginning token and eos token, as context for the NAR decoder.

The AR decoding generates one new token per iteration from left to right. The attention mask for the AR decoding procedure is shown in Table 2. For the first iteration, it predicts the first token y_1 with the position query \mathbf{p}_1 , using the context set to $[B]$ concatenated with $L + 1$ mask tokens. For the succeeding iteration i , the context is set to the determined tokens (i.e. $[B]$ together with the determined characters y_1 to y_{i-1}) concatenated with the mask tokens for the unpredicted part (i.e. $[M]_i$ to $[M]_{L+1}$). We use \mathbf{p}_i as the position query.

Before each refinement, the length is re-determined based on the predicted text from the previous iteration. When decoding a character y_i , the query \mathbf{p}_i can attend to all information from the previous iteration except the corresponding token y_i itself. Therefore, one mask token for this token, prepended with other determined tokens, is set as the context. For examples, when refining y_2 , the attention mask of $[[B], y_1, y_2, \dots, y_L, [E], [M]_0, [M]_1, [M]_2, \dots, [M]_L, [M]_{L+1}]$ is $[0, 0, 1, 0, 0, 0, 1, 1, 0, 1, 1, 1]$. Besides, all tokens are refined simultaneously.

4.3 Comparison with State-of-the-Art

We compare the proposed models with previous SOTA methods. Since these methods were evaluated on noisy benchmarks, in order to compare their true performance, we collect the available released pretrained models and directly evaluate them on the cleansed benchmark. For the PARSeq [3] model trained on the synthetic dataset, we reproduce the model following the official configuration. Additionally, since the original PIMNet [30] uses a CNN backbone, we reproduce it with the same small DeiT backbone for a fair comparison. The inference time is calculated on one NVIDIA Tesla V100 GPU, averaged over 7,672 benchmark images.

As demonstrated in Table 3, language-aware methods outperform language-free methods (such as TRBA [1] and ViTSTR [1]), highlighting the importance of linguistic knowledge in scene text recognition. When trained on synthetic datasets, our MPSTR model achieves comparable performance with SOTA methods. Remarkably, our method outperforms LevOCR [6] by 0.2% on the cleansed

Table 4: Recognition accuracy on more challenging datasets. The marks share the same meaning as in Table 3.

Method	Data	ArT	COCO	Uber	Average
PIMNet* [30]	S	69.2	59.6	41.0	50.3
ABINet [10]	S	68.1	63.1	39.5	49.3
LevOCR [6]	S	69.2	64.6	41.2	50.9
MGP-STR [†] [43]	S	68.1	63.3	40.5	50.1
PARSeq _N * [3]	S	68.6	63.3	40.4	50.1
PARSeq _A * [3]	S	69.4	64.5	41.7	51.3
MPSTR _N (Ours)	S	69.6	63.6	42.3	51.6
MPSTR _A (Ours)	S	69.9	64.5	42.8	52.1
PIMNet* [30]	R	81.0	73.5	80.2	79.9
PARSeq _N [3]	R	83.0	77.0	82.4	82.1
PARSeq _A [3]	R	84.5	79.8	84.5	84.1
MPSTR _N (Ours)	R	83.6	79.9	84.1	83.7
MPSTR _A (Ours)	R	84.4	80.3	84.9	84.4

benchmark, while using only a quarter of the parameters and one-third of the inference time.

Compared to the PLM-based method PARSeq trained on synthetic and real datasets, our AR decoding model outperforms the corresponding PARSeq model (PARSeq_A) with an average accuracy improvement of 0.6% and 0.3%, respectively. Meanwhile, the NAR model surpasses PARSeq_N with improvements of 0.7% and 0.9%. Notably, our NAR model MPSTR_N achieves comparable performance with PARSeq_A (93.3% vs. 93.3% for synthetic dataset and 97.2% vs. 97.1% for real dataset) while reducing latency by approximately 5ms. For the MLM-based method, our MPSTR_N achieves average improvements of 1.0% and 1.5% with NAR decoding compared to PIMNet trained on synthetic and real datasets, respectively. These results demonstrate the effectiveness and efficiency of our proposed MPSTR approach in scene text recognition.

4.4 Experiments on Challenging Datasets

Since the performance on benchmark datasets is close to saturation, we further compare our method with previous SOTA models on more challenging datasets, as shown in Table 4. Compared with the PLM-based PARSeq trained on synthetic or real datasets, our models outperform the corresponding PARSeq models. Specifically, the AR models MPSTR_A outperforms PARSeq trained on synthetic or real datasets with 0.7% or 0.3% improvement respectively. Furthermore, with the help of global linguistic information, our NAR models MPSTR_N trained on the two kinds of datasets achieve 1.3% and 1.6% improvements respectively on the average accuracy for the three challenging datasets. The results demonstrate that our proposed MPSTR method consistently outperforms or achieves comparable performance with the state-of-the-art methods across these challenging datasets, highlighting the robustness and effectiveness of our approach in handling difficult text recognition scenarios.

4.5 Ablation Study

4.5.1 Language Modeling Method. Table 5 presents an ablation study examining the contributions of different language modeling

Table 5: Ablation study on language modeling strategy. Baseline is ordinary left-to-right AR model. * indicates that the model is trained and evaluated with the GT lengths.

Method	Real Data		Synthetic Data	
	AR	NAR	AR	NAR
baseline	96.63	0.00	93.12	0.00
PLM	97.10	96.33	93.25	92.58
PLM+MLM	97.43	97.21	93.86	93.29
PLM+MLM*	97.71	97.67	94.44	94.18

Table 6: Ablation study of MLM integration. Mask token is appending mask tokens and length represents length supervision.

Mask Token	Length	Real Data		Synthetic Data	
		AR	NAR	AR	NAR
✓	✗	96.83	53.42	93.36	36.58
✗	✓	96.67	96.39	93.23	92.54
✓	✓	97.43	97.21	93.86	93.29

strategies. The baseline AR model relies on a single way left-to-right decoding, so it cannot permit NAR inference. Adding PLM (with a permutation number of 12, as in our MPSTR) enables NAR decoding by learning linguistic rules among characters. MLM further improves AR and NAR accuracy with global contextual information. Notably, NAR decoding models achieve more significant gains with the global positional information provided by MLM. As PLM alone does not provide valuable information except for the beginning token for the first MHCA between context and position; for instance, PARSeq_N predicts a redundant character "t" for the first image in Figure 5. We also provide an upper bound in the last row, where we use the ground truth word length to set the number of appending mask tokens. In summary, our unified language modeling method contributes to better context learning with global linguistic information and comprehensive dependencies among characters.

4.5.2 MLM Integration. We conducted an ablation study on the integration of MLM. From the results in row 1 of Table 6, we can observe that introducing mask tokens to the model without length supervision cannot allow NAR inference. It is intuitive since our unified likelihood formulated as equation (5) demands the positional information of unpredicted tokens at each decoding step. If we just add the predicted length embedding to the position query in the first MHCA, the performance is not satisfactory due to the imperfect length prediction. This implies that the integration of the MLM strategy means more than just the length; it can actually contribute to more sophisticated linguistic learning. Thus, to effectively unify PLM and MLM, both appending mask tokens and length information are required. As shown in the table, all models provide gains with this integration.

Table 7: Ablation study about length prediction methods.

Method	Real Data		Synthetic Data		Length	
	AR	NAR	AR	NAR	Real	Synth
Char-level	96.74	96.04	92.80	91.63	98.44	95.41
Word-level	97.43	97.21	93.86	93.29	98.79	96.41

Table 8: Recognition accuracy of MPSTR trained using real datasets on the benchmark vs the number of permutations used (K) for training. No perturbation is applied for these models. AR acc. and NAR acc. are evaluated without refinement. For cloze acc., we use GT label as the initial prediction.

K	AR acc.	NAR acc.	cloze acc.
1	96.18	0.00	63.23
2	96.58	1.32	97.54
6	96.23	96.10	98.00
12	96.65	96.32	98.08
18	96.45	96.34	97.97

Table 9: MPSTR_N's reconigntion results on the benchmark vs the ratio of images trained with perturbed length.

Data	0%	25%	33%	50%	66%	75%
S	92.09	92.47	92.55	92.74	93.10	92.80
R	96.72	96.81	97.21	96.73	-	-

4.5.3 *Word Length Prediction.* We analyze the performance of different length prediction methods. There are two intuitive approaches to predict length. One is determining whether each position has a character or not (*i.e.*, character-level prediction), and the other is predicting the length of words directly (*i.e.*, word-level prediction). To predict the length at the character-level, we employ a parallel decoder to perform binary classification for each position. The introduced length token represents word-level prediction taking the entire image into consideration. As demonstrated in Table 7, the word-level method surpasses the character-level approach, as it considers the global information. Consequently, we adopt the word-level [*len*] token prediction method.

4.5.4 *Permutation Number.* We investigate the impact of different permutation numbers K on the model performance. As demonstrated by the results in Table 8, the NAR decoding procedure struggles to work properly with few permutations ($K = 1, 2$), as the contextual information is limited. However, AR decoding performs very well because of the consistency between training and inference along with the length supervision. As K increases, both AR and NAR show improved performance when $K \leq 12$. Notably, MPSTR requires more permutations to achieve the best performance compared with PLM-based PARseq because of the additional global linguistic information introduced by padding mask tokens.

4.5.5 *Perturbation training.* To evaluate the effectiveness of perturbation training in improving the decoder's robustness for predicted

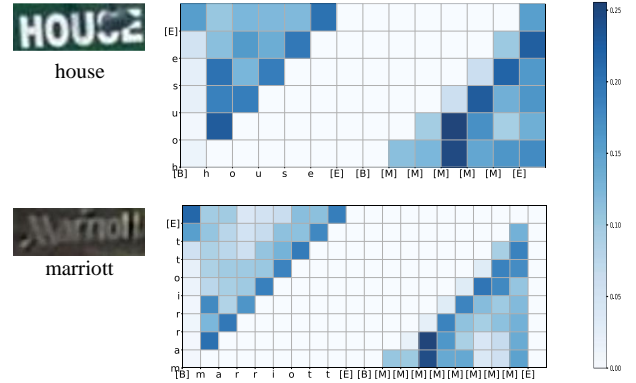


Figure 4: Visualization of the first MHCA's attention weights of MPSTR_A.

Images	AR	NAR	Images	AR	NAR
	mar-nott	mar-iottttt...		houce	houce
	marriott	mar-nott		house	house
	lounse	lounse		celebrazing	celebrazime
	lounge	lounge		celebrating	celebrating
	arald11930	arald11930		circ-as	circ-as
	arald11930	arald11930		circ-es	circ-es

Figure 5: Challenging examples that PARSeq fails (upper) but our MPSTR (bottom) improves performance or successes. "mari-iottttt..." stands for the redundancy of the last character "t".

lengths, we conduct an ablation study on the ratio of images trained with perturbed length. Since most synthetic text images are more regular compared to real ones, the performance of length prediction is relatively worse, leading to more perturbation during inference. As a result, the model trained on synthetic datasets requires more perturbed images (66%), as shown in Table 9. In contrast, the model trained on real datasets achieves highest performance with 33% perturbed images. Moreover, for models trained on real datasets, we do not conduct experiments with 66% and 75% perturbation ratios as its accuracy begins to decrease at 50%.

4.6 Qualitative Analysis

We visualize the MPSTR_A attention weights of the permuted and masked text in MP-decoder for two challenging examples that PARseq fails in Figure 4. As shown in this figure, MP-decoder could obtain not only previous characters' information, but also the information provided by padding mask tokens with specific length. For example, when decoding the first character, there is no determined characters expect the beginning token, but MP-decoder benefits from the mask tokens, where the third one contributes the most to both two images. Through training on several permutations of the original text, MPSTR could learn better internal language model with global linguistic information and build dependency among

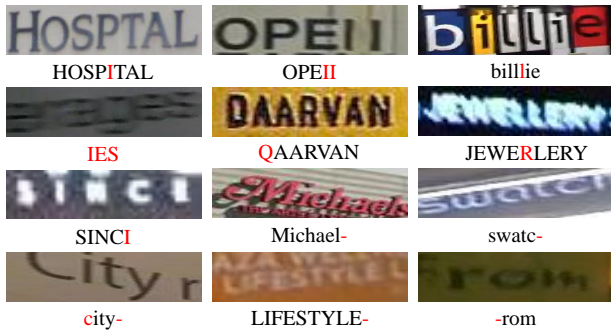


Figure 6: Examples of label noise in benchmark datasets, where the mislabeled characters are highlighted in color. A red dash (-) indicates a missing character.

every characters. Figure 5 shows that MPSTR provides more robust results on challenging examples compared with PARSeq.

5 CONCLUSION

In this paper, we propose the masked and permuted implicit context learning approach for scene text recognition to overcome the limitations of both PLM and MLM, while learning a more effective internal LM with global linguistic information. Additionally, word-level text length prediction is introduced to effectively integrate the MLM method and enhance the quality of contextual learning. Our proposed MPSTR achieves SOTA performance on most public benchmarks, validating the effectiveness of our approach. Furthermore, the consistent improvements in both AR and NAR decoding demonstrate the generalization capabilities of our proposed method.

A BENCHMARK CLEANSED

There are six widely-used public benchmarks: IIIT 5k-word (IIIT5k) [25], which comprises 3,000 high-quality website images; ICDAR 2013 (IC13) [18], containing either 1,015 or 857 images (the latter excludes images with words less than three characters); Street View Text (SVT) [42], consisting of 647 images from the Google Street View; ICDAR 2015 (IC15) [17] featuring 2,077 unfocused images captured by Google Glass (some researchers use a 1,811-image version that omits extremely distorted images); SVT-Perspective (SVTP) [29], with 645 test word images from the Google Street View; and CUTE80 (CUTE) [32], which includes 288 high-quality curved images.

Despite the widespread use of these existing benchmarks in scene text recognition, we have noticed that there are mislabeled images in the benchmark. Although [2] provided a version of cleansed labels for benchmark datasets, there are still several mislabeled images, as illustrated by the examples in Figure 6. We conduct further verification of these labels. The mislabeled examples can be classified into three types: missing character, alphabetic error, and completely wrong. We will provide the cleansed benchmark datasets to ensure a more accurate evaluation of scene text recognition models.

REFERENCES

- [1] Rowel Atienza. 2021. Vision transformer for fast and efficient scene text recognition. In *International Conference on Document Analysis and Recognition*. Springer, 319–334.
- [2] Jeonghun Baek, Geewook Kim, Junyeop Lee, Sungrae Park, Dongyoon Han, Sangdoon Yun, Seong Joon Oh, and Hwalsuk Lee. 2019. What is wrong with scene text recognition model comparisons? dataset and model analysis. In *Proceedings of the IEEE/CVF international conference on computer vision*. 4715–4723.
- [3] Darwin Bautista and Rowel Atienza. 2022. Scene Text Recognition with Permuted Autoregressive Sequence Models. In *European Conference on Computer Vision*. Springer, 178–196.
- [4] Xiaoxue Chen, Lianwen Jin, Yuanzhi Zhu, Canjie Luo, and Tianwei Wang. 2021. Text recognition in the wild: A survey. *ACM Computing Surveys (CSUR)* 54, 2 (2021), 1–35.
- [5] Chee Kheng Chng, Yuliang Liu, Yipeng Sun, Chun Chet Ng, Canjie Luo, Zihan Ni, ChuanMing Fang, Shuaitao Zhang, Junyu Han, Errui Ding, et al. 2019. Icdar2019 robust reading challenge on arbitrary-shaped text-rrc-art. In *2019 International Conference on Document Analysis and Recognition (ICDAR)*. IEEE, 1571–1576.
- [6] Cheng Da, Peng Wang, and Cong Yao. 2022. Levenshtein OCR. In *European Conference on Computer Vision*. Springer, 322–338.
- [7] Jacob Devlin, Ming-Wei Chang, Kenton Lee, and Kristina Toutanova. 2018. Bert: Pre-training of deep bidirectional transformers for language understanding. *arXiv preprint arXiv:1810.04805* (2018).
- [8] Alexey Dosovitskiy, Lucas Beyer, Alexander Kolesnikov, Dirk Weissenborn, Xi-aohua Zhai, Thomas Unterthiner, Mostafa Dehghani, Matthias Minderer, Georg Heigold, Sylvain Gelly, et al. 2020. An image is worth 16x16 words: Transformers for image recognition at scale. *arXiv preprint arXiv:2010.11929* (2020).
- [9] Yongkun Du, Zhineng Chen, Caiyan Jia, Xiaoting Yin, Tianlun Zheng, Chenxia Li, Yuning Du, and Yu-Gang Jiang. 2022. SVTR: Scene Text Recognition with a Single Visual Model. In *Proceedings of the 31st International Joint Conference on Artificial Intelligence*. 884–890.
- [10] Shancheng Fang, Hongtao Xie, Yuxin Wang, Zhendong Mao, and Yongdong Zhang. 2021. Read like humans: Autonomous, bidirectional and iterative language modeling for scene text recognition. In *Proceedings of the IEEE/CVF Conference on Computer Vision and Pattern Recognition*. 7098–7107.
- [11] Alex Graves, Santiago Fernández, Faustino Gomez, and Jürgen Schmidhuber. 2006. Connectionist temporal classification: labelling unsegmented sequence data with recurrent neural networks. In *Proceedings of the 23rd international conference on Machine learning*. 369–376.
- [12] Tongkun Guan, Chaochen Gu, Jingzheng Tu, Xue Yang, and Qi Feng. 2022. A Glyph-driven Topology Enhancement Network for Scene Text Recognition. *arXiv preprint arXiv:2203.03382* (2022).
- [13] Ankush Gupta, Andrea Vedaldi, and Andrew Zisserman. 2016. Synthetic data for text localisation in natural images. In *Proceedings of the IEEE conference on computer vision and pattern recognition*. 2315–2324.
- [14] Wenyang Hu, Xiaocong Cai, Jun Hou, Shuai Yi, and Zhiping Lin. 2020. Gtc: Guided training of ctc towards efficient and accurate scene text recognition. In *Proceedings of the AAAI Conference on Artificial Intelligence*, Vol. 34. 11005–11012.
- [15] Max Jaderberg, Karen Simonyan, Andrea Vedaldi, and Andrew Zisserman. 2016. Reading text in the wild with convolutional neural networks. *International journal of computer vision* 116, 1 (2016), 1–20.
- [16] Hui Jiang, Yunlu Xu, Zhanzhan Cheng, Shiliang Pu, Yi Niu, Wenqi Ren, Fei Wu, and Wenming Tan. 2021. Reciprocal feature learning via explicit and implicit tasks in scene text recognition. In *Document Analysis and Recognition-ICDAR 2021: 16th International Conference, Lausanne, Switzerland, September 5–10, 2021, Proceedings, Part I*. Springer, 287–303.
- [17] Dimosthenis Karatzas, Lluís Gomez-Bigorda, Angelos Nicolaou, Suman Ghosh, Andrew Bagdanov, Masakazu Iwamura, Jiri Matas, Lukas Neumann, Vijay Ramaseshan Chandrasekhar, Shijian Lu, et al. 2015. ICDAR 2015 competition on robust reading. In *2015 13th international conference on document analysis and recognition (ICDAR)*. IEEE, 1156–1160.
- [18] Dimosthenis Karatzas, Faisal Shafait, Seiichi Uchida, Masakazu Iwamura, Lluís Gomez i Bigorda, Sergi Robles Mestre, Joan Mas, David Fernandez Mota, Jon Almazan Almazan, and Lluís Pere De Las Heras. 2013. ICDAR 2013 robust reading competition. In *2013 12th international conference on document analysis and recognition*. IEEE, 1484–1493.
- [19] Bohan Li, Ye Yuan, Dingkang Liang, Xiao Liu, Zhilong Ji, Jinfeng Bai, Wenyu Liu, and Xiang Bai. 2022. When Counting Meets HMER: Counting-Aware Network for Handwritten Mathematical Expression Recognition. In *Computer Vision-ECCV 2022: 17th European Conference, Tel Aviv, Israel, October 23–27, 2022, Proceedings, Part XXVIII*. Springer, 197–214.
- [20] Hui Li, Peng Wang, Chunhua Shen, and Guyu Zhang. 2019. Show, attend and read: A simple and strong baseline for irregular text recognition. In *Proceedings of the AAAI conference on artificial intelligence*. 8610–8617.
- [21] Minghui Liao, Jian Zhang, Zhaoyi Wan, Fengming Xie, Jiajun Liang, Pengyuan Lyu, Cong Yao, and Xiang Bai. 2019. Scene text recognition from two-dimensional perspective. In *Proceedings of the AAAI Conference on Artificial Intelligence*, Vol. 33.

- 8714–8721.
- [22] Wei Liu, Chaofeng Chen, Kwan-Yee K Wong, Zhizhong Su, and Junyu Han. 2016. Star-net: a spatial attention residue network for scene text recognition.. In *BMVC*, Vol. 2. 7.
- [23] Shangbang Long, Xin He, and Cong Yao. 2021. Scene text detection and recognition: The deep learning era. *International Journal of Computer Vision* 129, 1 (2021), 161–184.
- [24] Stephen Merity, Caiming Xiong, James Bradbury, and Richard Socher. 2017. Pointer Sentinel Mixture Models. In *International Conference on Learning Representations*. <https://openreview.net/forum?id=Byj72udxe>
- [25] Anand Mishra, Karteek Alahari, and CV Jawahar. 2012. Scene text recognition using higher order language priors. In *BMVC-British machine vision conference*. BMVA.
- [26] Byeonghu Na, Yoonsik Kim, and Sungrae Park. 2022. Multi-modal text recognition networks: Interactive enhancements between visual and semantic features. In *European Conference on Computer Vision*. Springer, 446–463.
- [27] Fatemeh Naemi, Vahid Ghods, and Hassan Khalesi. 2022. Scene text detection and recognition: a survey. *Multimedia Tools and Applications* (2022), 1–36.
- [28] Lukáš Neumann and Jiří Matas. 2012. Real-time scene text localization and recognition. In *2012 IEEE conference on computer vision and pattern recognition*. IEEE, 3538–3545.
- [29] Trung Quy Phan, Palaiahnakote Shivakumara, Shangxuan Tian, and Chew Lim Tan. 2013. Recognizing text with perspective distortion in natural scenes. In *Proceedings of the IEEE International Conference on Computer Vision*. 569–576.
- [30] Zhi Qiao, Yu Zhou, Jin Wei, Wei Wang, Yuan Zhang, Ning Jiang, Hongbin Wang, and Weiping Wang. 2021. PIMNet: a parallel, iterative and mimicking network for scene text recognition. In *Proceedings of the 29th ACM International Conference on Multimedia*. 2046–2055.
- [31] Zhi Qiao, Yu Zhou, Dongbao Yang, Yucan Zhou, and Weiping Wang. 2020. Seed: Semantics enhanced encoder-decoder framework for scene text recognition. In *Proceedings of the IEEE/CVF Conference on Computer Vision and Pattern Recognition*. 13528–13537.
- [32] Anhar Risnumawan, Palaiahankote Shivakumara, Chee Seng Chan, and Chew Lim Tan. 2014. A robust arbitrary text detection system for natural scene images. *Expert Systems with Applications* 41, 18 (2014), 8027–8048.
- [33] Baoguang Shi, Xiang Bai, and Cong Yao. 2016. An end-to-end trainable neural network for image-based sequence recognition and its application to scene text recognition. *IEEE transactions on pattern analysis and machine intelligence* 39, 11 (2016), 2298–2304.
- [34] Baoguang Shi, Mingkun Yang, Xinggang Wang, Pengyuan Lyu, Cong Yao, and Xiang Bai. 2018. Aster: An attentional scene text recognizer with flexible rectification. *IEEE transactions on pattern analysis and machine intelligence* 41, 9 (2018), 2035–2048.
- [35] Leslie N Smith and Nicholay Topin. 2019. Super-convergence: Very fast training of neural networks using large learning rates. In *Artificial intelligence and machine learning for multi-domain operations applications*, Vol. 11006. SPIE, 369–386.
- [36] Kaitao Song, Xu Tan, Tao Qin, Jianfeng Lu, and Tie-Yan Liu. 2020. Mpnnet: Masked and permuted pre-training for language understanding. *Advances in Neural Information Processing Systems* 33 (2020), 16857–16867.
- [37] Yew Lee Tan, Adams Wai-Kin Kong, and Jung-Jae Kim. 2022. Pure Transformer with Integrated Experts for Scene Text Recognition. In *European Conference on Computer Vision*. Springer, 481–497.
- [38] Hugo Touvron, Matthieu Cord, Matthijs Douze, Francisco Massa, Alexandre Sablayrolles, and Hervé Jégou. 2021. Training data-efficient image transformers & distillation through attention. In *International Conference on Machine Learning*. PMLR, 10347–10357.
- [39] Ashish Vaswani, Noam Shazeer, Niki Parmar, Jakob Uszkoreit, Llion Jones, Aidan N Gomez, Łukasz Kaiser, and Illia Polosukhin. 2017. Attention is all you need. *Advances in neural information processing systems* 30 (2017).
- [40] Andreas Veit, Tomas Matera, Lukas Neumann, Jiri Matas, and Serge Belongie. 2016. Coco-text: Dataset and benchmark for text detection and recognition in natural images. *arXiv preprint arXiv:1601.07140* (2016).
- [41] Zhaoyi Wan, Minghang He, Haoran Chen, Xiang Bai, and Cong Yao. 2020. Textscanner: Reading characters in order for robust scene text recognition. In *Proceedings of the AAAI conference on artificial intelligence*, Vol. 34. 12120–12127.
- [42] Kai Wang, Boris Babenko, and Serge Belongie. 2011. End-to-end scene text recognition. In *2011 International conference on computer vision*. IEEE, 1457–1464.
- [43] Peng Wang, Cheng Da, and Cong Yao. 2022. Multi-granularity Prediction for Scene Text Recognition. In *European Conference on Computer Vision*. Springer, 339–355.
- [44] Yuxin Wang, Hongtao Xie, Shancheng Fang, Jing Wang, Shenggao Zhu, and Yongdong Zhang. 2021. From two to one: A new scene text recognizer with visual language modeling network. In *Proceedings of the IEEE/CVF International Conference on Computer Vision*. 14194–14203.
- [45] Yuxin Wang, Hongtao Xie, Shancheng Fang, Mengting Xing, Jing Wang, Shenggao Zhu, and Yongdong Zhang. 2022. PETR: Rethinking the Capability of Transformer-Based Language Model in Scene Text Recognition. *IEEE Transactions on Image Processing* 31 (2022), 5585–5598.
- [46] Zecheng Xie, Yaoxiong Huang, Yuanzhi Zhu, Lianwen Jin, Yuliang Liu, and Lele Xie. 2019. Aggregation cross-entropy for sequence recognition. In *Proceedings of the IEEE/CVF conference on computer vision and pattern recognition*. 6538–6547.
- [47] Zhilin Yang, Zihang Dai, Yiming Yang, Jaime Carbonell, Russ R Salakhutdinov, and Quoc V Le. 2019. Xlnet: Generalized autoregressive pretraining for language understanding. *Advances in neural information processing systems* 32 (2019).
- [48] Cong Yao, Xiang Bai, Baoguang Shi, and Wenyu Liu. 2014. Strokelets: A learned multi-scale representation for scene text recognition. In *Proceedings of the IEEE conference on computer vision and pattern recognition*. 4042–4049.
- [49] Qixiang Ye and David Doermann. 2014. Text detection and recognition in imagery: A survey. *IEEE transactions on pattern analysis and machine intelligence* 37, 7 (2014), 1480–1500.
- [50] Deli Yu, Xuan Li, Chengquan Zhang, Tao Liu, Junyu Han, Jingtuo Liu, and Errui Ding. 2020. Towards accurate scene text recognition with semantic reasoning networks. In *Proceedings of the IEEE/CVF Conference on Computer Vision and Pattern Recognition*. 12113–12122.
- [51] Ying Zhang, Lionel Gueguen, Ilya Zharkov, Peter Zhang, Keith Seifert, and Ben Kadlec. 2017. Uber-text: A large-scale dataset for optical character recognition from street-level imagery. In *SUNw: Scene Understanding Workshop-CVPR*, Vol. 2017. 5.
- [52] Yingying Zhu, Cong Yao, and Xiang Bai. 2016. Scene text detection and recognition: Recent advances and future trends. *Frontiers of Computer Science* 10, 1 (2016), 19–36.